GLASS TRANSITION

Operational Definition

At a relatively simple-minded practical and operational (and thus theoretically nonrigorous) level of treatment, we can define (1) the *glass-transition temperature* (T_g) as the temperature at which the forces holding the distinct components of an amorphous solid together are overcome by thermally induced motions within the time scale of the experiment, so that these components are able to undergo large-scale molecular motions on this time scale, limited mainly by the inherent resistance of each component to such flow. The practical effects of the glass transition on the processing and performance characteristics of polymers are implicit in this definition.

In most polymeric as well as nonpolymeric amorphous materials, the ability to undergo large-scale molecular motions implies the freedom to flow, so that the material becomes a fluid above T_g. However, in the special class of polymers commonly described as "thermosets," covalent cross-links limit the ability to undergo large-scale deformation. Consequently, above T_g, thermosets become "elastomers" (also known as "cross-linked rubbers").

On the experimental time scale, above T_g, nonthermoset amorphous materials are viscous fluids. Their glass transitions can then be viewed as transitions, over the experimental time scale, from predominantly elastic "solid-like" to predominantly viscous "liquid-like" behavior. In fact, traditionally, the glass transition has often been identified in practical terms (not only for polymers, but also for amorphous inorganic materials) as taking place when the viscosity reaches a threshold value (most commonly taken to be 10^{13} P). The glass transition occurs in the reverse direction if the temperature is instead lowered from above to below T_g, with the material then undergoing "vitrification." Again with the

exception of thermosets, this reverse transition upon cooling can be described as going from viscous to elastic behavior. For every glass former, there is a temperature-dependent frequency f (T), and a time scale $t(T)=1/f$ (T), such that at frequencies higher than f the system is elastic and for lower frequencies it is viscous.

In thermosets large-scale molecular motions also become possible above T_g, but these motions are limited by the cross-links that serve as topological constraints for the chain segments between them. (The chain segments between cross-links are the "distinct components" for such materials). The general operational definition given above, therefore, remains valid. However, the specimen as a whole does not and cannot undergo large-scale viscous flow. In fact, it may instead exhibit strongly elastic behavior above T_g because of the presence of the network junctions. The glass transition, therefore, involves the onset of large-scale motions (in other words, "viscous" behavior) on the molecular scale in all amorphous materials. However, on a larger length scale, in thermosets, it cannot be described as occurring between predominantly elastic and predominantly viscous behavior. In the remainder of this article, whenever the glass transition is described in terms of its effect on the viscosity in large-scale flows, it should be understood that thermosets and elastomers are being excluded from the scope of the discussion.

Experimental Methods and Modeling

Several well-established experimental methods are available to measure T_g. The tabulated data are subject to many uncertainties. These uncertainties include the use of different experimental methods, ill-characterized differences between samples in terms of their precise composition and thermal history, and the nonequilibrium (kinetic) aspect of the glass transition which introduces an inherent rate dependence. It is, therefore, best to compare T_g values by using data obtained with the same experimental method for well-characterized samples, whenever possible.

Many theories based on thermodynamic and kinetic considerations, as well as many quantitative structure–property relationships with different amounts of empiricism, have been developed for T_g as a result of decades of research. Further work along these directions can be expected to result only in incremental improvements in fundamental understanding and predictive ability. The rapidly increasing power of computational hardware and software has encouraged attempts to study the glass transition by fully atomistic or coarse-grained numerical simulations, and significant progress may be expected along this exciting new research frontier in coming years.

Practical Importance and Common Methods for Measurement

The glass transition is by far the most important one among the many transitions and relaxations (2) observed in amorphous polymers. When an amorphous polymer undergoes the glass transition, almost all of its properties that relate to its processing and/or performance change dramatically. These changes are important both in determining the processing and performance characteristics of polymers,

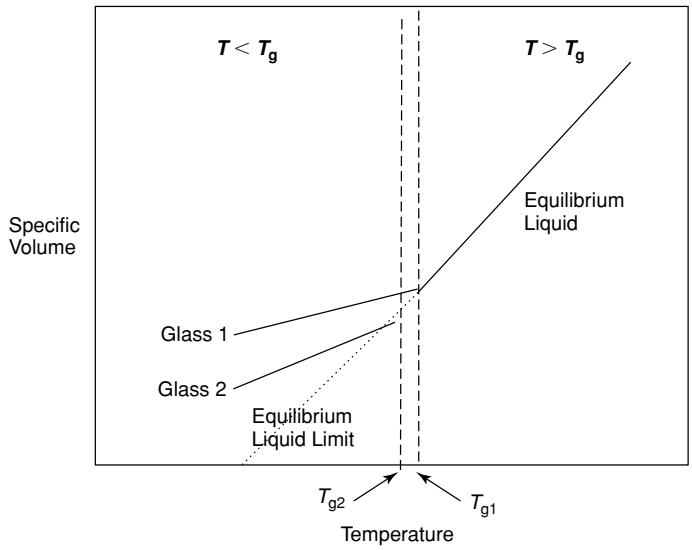

Fig. 1. Schematic illustration of temperature dependences of specific volumes of amorphous materials. This figure also illustrates the effects of the nonequilibrium nature of glass structure, which results from kinetic factors. Glass 1 and Glass 2 are specimens of the same polymer, but subjected to different thermal histories. For example, Glass 1 may have been quenched from the melt very rapidly, while Glass 2 may either have been cooled slowly or subjected to volumetric relaxation via annealing in the glassy state.

and in the selection of suitable methods for measuring the value of T_g itself. The following are some important examples of the effects of going through T_g, as well as of the common methods for measuring T_g based on these effects (1).

The temperature dependence of the specific volume (1/density) of an amorphous material is shown schematically in Figure 1. The coefficient of thermal expansion (rate of change of specific volume with temperature) increases from its value for the "glassy" polymer to its typically much larger value for the "rubbery" polymer when the temperature increases from below to above T_g. The rate of decrease of the density with increasing temperature then becomes much faster above T_g. However, unlike melting where there is a discontinuity in the specific volume itself, the specific volume is a continuous function of the temperature at T_g; only its slope changes in going through the glass transition. Figure 1 also illustrates the effects of the nonequilibrium nature of glass structure, which results from kinetic factors, as will be discussed further later in this article. The effect of T_g on the coefficient of thermal expansion enables its measurement by *dilatometry*.

The dependence of the specific heat capacity of an amorphous polymer on the temperature is shown schematically in Figure 2. The heat capacity of an amorphous polymer jumps from its value for the "solid" polymer to its significantly larger value for the "liquid" (molten or rubbery) polymer at T_g. However, unlike melting where there is a discontinuity in the enthalpy, the enthalpy is a continuous function of the temperature at T_g; only its slope changes in going through the glass transition. The effect of T_g on the heat capacity enables its measurement by *differential scanning calorimetry*, which is by far the most commonly used method to measure it.

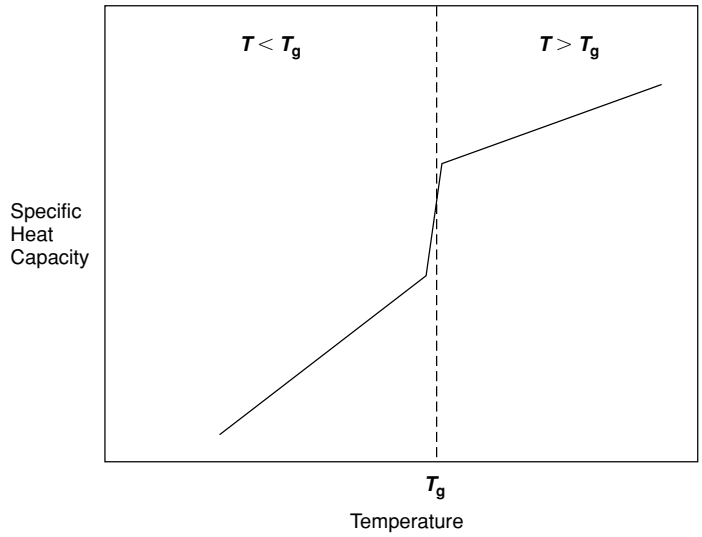

Fig. 2. Schematic illustration of temperature dependences of specific heat capacities of amorphous polymers. The heat capacity "jumps" to a much higher value over a narrow temperature range as the polymer goes through the glass transition. It increases more slowly with increasing temperature above T_g than it did below T_g.

An amorphous polymer typically "softens" drastically as its temperature is raised above T_g, so that its structural rigidity is lost. At the typical time scale of a practical observation, the key indicators of stiffness (the tensile and shear moduli), which decrease very slowly with increasing temperature below T_g, decrease rapidly over a narrow temperature range with further increase in temperature by several (sometimes up to three or even four) orders of magnitude upon traversing T_g. The typical behavior of the tensile (Young's) or shear modulus upon going through the glass transition is compared for a linear (physically entangled but not chemically cross-linked) amorphous polymer, a chemically cross-linked amorphous polymer, and a semicrystalline polymer, in the schematic drawings shown in Figure 3. [However, strictly speaking, this summary is an oversimplification. The elastic moduli for elastic frequencies are not sharp functions of T. The apparent changes are due to the change of f (T) when one works at the time scale of the experiment.] The yield stress also decreases rapidly upon traversing T_g, going to zero slightly above T_g. These changes in the mechanical properties, from "glassy" (below T_g), to "leathery" (in the immediate vicinity of T_g), to "rubbery" (above T_g), have strong implications in terms of practical applications of polymers. These changes also enable the use of mechanical testing methods to measure T_g. Among such methods, *dynamic mechanical spectroscopy*, which measures the viscoelastic characteristics of a polymer under mechanical deformation, is the most reliable and most widely utilized one.

It is worth noting that, in practice, the "heat distortion temperature" (3) is used more often than T_g in the product literature of commercial polymers as an indicator of the mechanical softening temperature. It is closely related to (usually slightly lower than) T_g for amorphous polymers.

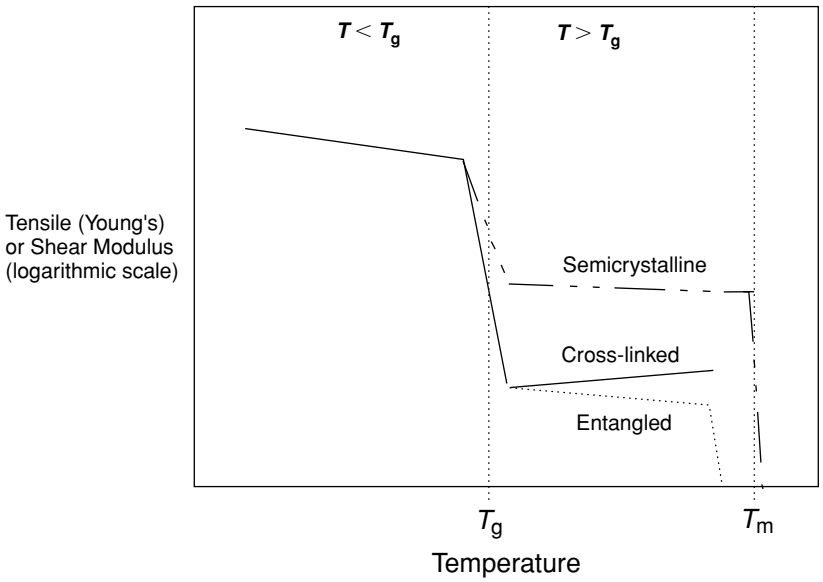

Fig. 3. Schematic illustration of typical behavior of tensile (Young's) and shear moduli upon going through the glass transition. Linear (physically entangled but not chemically cross-linked) amorphous polymers, chemically cross-linked amorphous polymers, and semicrystalline polymers are compared. These two moduli decrease slowly for $T < T_g$, and then drop rapidly over a narrow temperature range as the temperature increases above T_g. The drop may be up to 4 orders of magnitude for amorphous polymers, while it is smaller for semicrystalline polymers. The slight gradual increase in the modulus of the chemically cross-linked polymers above T_g is a result of entropic effects, as described by rubber elasticity theory, and persists until T is raised sufficiently for the polymer to undergo degradation. The gradual decrease in the modulus of a physically entangled polymer over the "rubbery plateau," followed by a precipitous drop into the "terminal zone" where the polymer becomes fluid-like, is due to increasing slippage of labile entanglement junctions. The crystallites in a semicrystalline polymer may provide a wide rubbery plateau regime if $T_m \gg T_g$, and the polymer then becomes fluid-like above T_m.

The rates of change (slopes of the curves) of many important properties (such as the refractive index, surface tension, and gas permeabilities) as a function of temperature, the value of the dielectric constant, and many other optical and electrical properties, often change considerably at T_g. These changes enable the measurement of T_g by using techniques such as *refractometry* and *dielectric relaxation spectroscopy*. Refractometry provides results which are similar to those obained from dilatometry because of the correlation between the rates of change of the specific volume and of the refractive index with temperature. Dielectric relaxation spectroscopy is based on general physical principles which are similar to those in dynamic mechanical spectroscopy, the main difference being in its use of an electrical rather than a mechanical stimulus.

In considering the methods summarized above for measuring T_g, it is important to note that, as discussed later in greater detail, the observed value of T_g can be affected significantly by kinetic factors. T_g is, therefore, dependent on the measurement rate. For example, the T_g measured by differential scanning calorimetry can be increased significantly by increasing the heating rate or by decreasing the

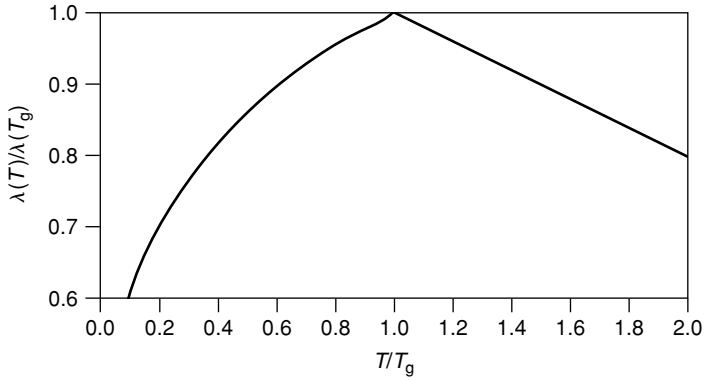

Fig. 4. Approximate form of the temperature dependence of the thermal conductivity $\lambda(T)$ of amorphous polymers, showing that it goes through its maximum value at T_g.

cooling rate during a calorimetric scan. Furthermore, the glass transition does not occur at a single sharply defined temperature but instead over a range of temperatures. There is often confusion in the literature about which point in that range (its onset, midpoint, or end) to use as the value of T_g. Similarly, the glass-transition range depends both on the rate (frequency) of measurement and on whether the specimen is being heated or cooled, in measuring T_g by dynamic mechanical spectroscopy or by dielectric relaxation spectroscopy. The typical temperature and/or frequency scanning rates used most often in different types of experiments also differ significantly. It is worth remembering, therefore, that not only are there many different methods for measuring T_g, but each method only gives a range of temperatures over which the glass transition occurs, and the T_g range measured by any one method can also vary because of the use of different testing conditions.

The thermal conductivity of a completely amorphous polymer goes through its maximum value at T_g, as illustrated in Figure 4.

The melt viscosity above T_g is typically lower than the viscosity in the glassy state below T_g by more than 10 orders of magnitude. Melt processing by techniques such as extrusion, injection molding, and compression molding requires temperatures significantly above T_g. If T_g is expressed in Kelvin, the optimum melt-processing temperature is normally at least $1.2T_g$. The general form of the dependence of the zero-shear melt viscosities η_0 of amorphous polymers as a function of the temperature is illustrated schematically in Figure 5. It is seen that η_0 has a non-Arrhenius "universal" shape for $T_g \leq T \leq 1.2T_g$, where the "reduced temperature" T/T_g roughly serves as the "corresponding states" variable. This universal behavior is lost above $1.2T_g$. The curves for different polymers separate from each other. For $T \gg 1.2T_g$, an Arrhenius-like (activated flow) regime is approached asymptotically. The activation energy in the extrapolation to the hypothetical limit of $T \to \infty$ depends on the chemical structure of the polymer.

One of the many practical uses of T_g is in characterizing polymer blends. When polymers with significantly different T_g values are blended, the effects on T_g often provide a useful indication of the extent of relative miscibility. For example, suppose that two polymers with T_g values of T_{g1} and T_{g2} (where $T_{g1} < T_{g2}$) are blended. If the blend manifests two distinct T_g values, near T_{g1} and T_{g2},

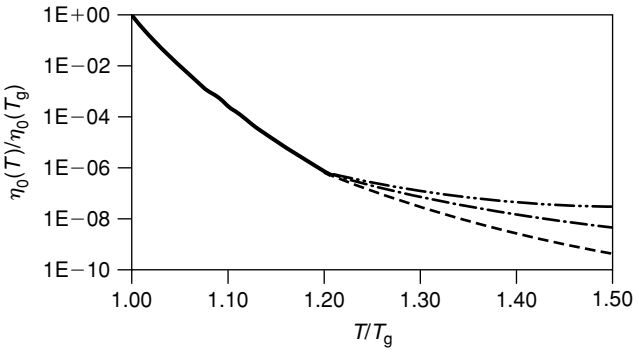

Fig. 5. Schematic illustration of general form of temperature dependence of zero-shear melt viscosities η_0 of amorphous polymers. It is seen that η_0 has a non-Arrhenius "universal" shape for $T_g \leq T \leq 1.2T_g$, where the "reduced temperature" T/T_g serves as the "corresponding states" variable. This universal behavior is lost above $1.2T_g$. The curves for different polymers separate from each other, as shown below for three polymers. For $T \gg 1.2T_g$, an Arrhenius-like (activated flow) regime is approached asymptotically. The activation energy in the extrapolation to the hypothetical limit of infinite temperature depends on the chemical structure of the polymer.

with relative intensities corresponding to the volume fractions of the components, this result usually implies that the polymers are immiscible and separated into macroscale phase domains. If the two glass transitions are broader than those observed for the individual polymers, and/or if the T_g values in the blend (T_g^{g1} and T_g^{g2}) fall between those of the polymers ($T_{g1} < T_g^{g1} < T_g^{g2} < T_{g2}$), this result usually indicates some intermixing of the polymers. If a single T_g value in the range of $T_{g1} < T_g < T_{g2}$ is observed and its position is correlated strongly with the volume fractions of the polymers, this result usually indicates that the polymers are miscible over the volume fraction range where such a single T_g value is observed. However, the use of T_g measurements to assess miscibility is subject to pitfalls, such as whether the T_g's differ sufficiently to allow resolution by a given measurement method, and whether the phase domains in a particular multiphase system are large enough for their effects on T_g to be detectable with that experimental technique (4).

Another practical use of T_g is in characterizing blends of polymers with small molecules. Over the industrially important blend composition ranges where the small molecules are dissolved in a polymeric matrix, such blends are usually referred to as *plasticized polymers*.

The glass transition also plays a major role in determining both the physical properties and the processing characteristics of semicrystalline polymers. Amorphous portions "melt" or "soften" at T_g. Crystalline portions remain "solid" up to the melting temperature T_m. (In practice, usually a semicrystalline polymer contains crystallites over a range of sizes and correspondingly a range of T_m values.) A semicrystalline polymer can be considered as a solid below T_g, as a composite consisting of solid and rubbery phases above T_g but below T_m, and as a fluid above T_m. The effect of the glass transition on the physical properties of semicrystalline polymers decreases with increasing crystallinity. Crystallization upon cooling from the

melt (from $T > T_m$) occurs over the range of $T_g < T < T_m$. Several industrially important fabrication processes (such as thermoforming, blow molding, and preparation of biaxially oriented films) take advantage of this crystallization temperature range, in manufacturing articles with the desired semicrystalline morphologies.

Thermoplastic elastomers (TPEs) (5) are multiphase polymers which behave like elastomers over a wide temperature range, but which can be melt-processed after raising the temperature sufficiently. They are used in many applications. Many TPEs are semicrystalline, with their practical use temperatures ranging from a lower limit of T_g (below which the amorphous phase solidifies so that the elastomeric behavior is lost) to an upper limit of T_m (above which the specimen becomes a viscous fluid so that its structural integrity is lost); see Figure 3. (The crystallites in such TPEs can thus be imagined to behave like meltable cross-links.) Many other TPEs are completely amorphous, with a use temperature range of T_{g1} (for lower-T_g phase) to T_{g2} (for higher T_g phase). On the other hand, certain families of thermoplastic elastomers have sharp glass transitions near room temperature and manifest reversible changes of up to 3 orders of magnitude in stiffness in going through T_g. These materials are known as *shape memory polymers* (6,7). These attributes make them ideally suited for some important specialized applications such as catheters which are rigid when handled by a surgeon outside the human body at room temperature (25°C), but flexible when inserted into the body (∼37°C).

Key Physical Aspects

Despite its apparent simplicity, the operational definition of T_g given earlier comprehends both of the key aspects of the physics of the glass transition. It states that, when a solid is heated up to T_g, it acquires enough thermal energy to be able to overcome two types of resistance to the large-scale motions of its components (1):

(1) The *cohesive forces* holding its different components together. The relevant components for the glass transition in amorphous polymers are chain segments. The cohesive forces can be quantified in terms of properties such as the cohesive energy density or the solubility parameter (square root of cohesive energy density).

(2) Attributes of the individual components (chain segments in polymers) which resist viscous flow. Resistance to the viscous flow of polymer chain segments is related to the topological and geometrical arrangement of their atoms, especially as expressed by the somewhat nebulous concept of *chain stiffness*. The glass transition occurs when there is enough freedom of motion for chain segments of up to several "statistical chain segments" (Kuhn segments) in length to be able to execute cooperative motions (8,9). As a general rule, the length of the Kuhn segment increases with increasing chain stiffness. See the two classic textbooks by Flory (10,11) for background information on statistical chain segments and on other configurational properties of polymer chains.

The effects of chain stiffness and cohesive forces on the value of T_g are different from each other. The "intrachain" effect of the stiffness of individual chain segments is generally (but not always) somewhat more important than the "interchain" effect of the cohesive (attractive) forces between different chains in determining the value of T_g.

Fundamental Theoretical Considerations

Based on the considerations summarized in previous section, it is not surprising to find that most theories of the glass transition (12–30) describe this phenomenon, either explicitly or implicitly, in terms of key physical ingredients whose values strongly depend on the chain stiffness and/or the cohesive forces. These theoretical treatments invariably treat the observed value of T_g as a kinetic (rate-dependent) manifestation of an underlying thermodynamic phenomenon. However, they differ significantly in their description of the nature of this phenomenon at a fundamental level.

Differences of opinion exist concerning the issue of whether or not the discontinuities observed at T_g in the second derivatives of the Gibbs free energy (ie, the coefficient of thermal expansion and the heat capacity) justify referring to the glass transition as a "second-order phase transition". It is important to note that the observed value of T_g is a function of the rate of measurement. For example, when the glass transition is approached from below, heating a specimen very quickly results in a higher apparent T_g than heating it very slowly. Conversely, when the glass transition is approached from above, cooling a specimen very quickly results in a lower apparent T_g than cooling it very slowly (see Fig. 1). There is, therefore, obviously, an important rate-dependent (kinetic) aspect of the glass transition. Nonetheless, it appears that the glass transition may also have an underlying fundamental thermodynamic basis. In other words, there is always a *thermodynamic equilibrium state*, defined as the state which has the lowest possible Gibbs free energy. Therefore, a thermodynamic driving force (preference for achieving as low a free energy as possible) must exist toward that equilibrium state. However, at the prevailing conditions of temperature and pressure, the approach toward that thermodynamic equilibrium state is so slow that the material seems to be "frozen" into a thermodynamically metastable glassy state. Consequently, *the consideration of the glass transition as a kinetic manifestation of an underlying thermodynamic phenomenon provides a reasonable fundamental physical framework for theories of the glass transition.*

The most essential aspects of this interplay of kinetics and thermodynamics are that (*1*) the glass transition involves freezing–defreezing phenomena, (*2*) one sees no sharp change in the parameters describing the static structure (such as the density and the structure factors) relative to the fluid after the vitrification event, and (*3*) what is a glassy material over a short time scale becomes a fluid over a sufficiently long time scale. (Sometimes, "sufficiently long" may mean millions of years, as in some geological phenomena.) The real mystery of the glass transition is in the acceleration of freezing (fragility) that makes the frequency $f(T)$ depend more strongly on the temperature than would be expected from a simple Arrhenius-type activated flow theory.

Quantitative Structure–Property Relationships

It is often important, especially in developing polymers for industrial applications, to be able to predict, rapidly, rough values for T_g as well as the probable trends between structural variants within and between polymer families. There is a long tradition of using quantitative structure–property relationships, developed by the statistical analysis of experimental data to express T_g as a function of (hopefully well-selected) compositional and structural descriptors, for such calculations. All such correlations either explicitly or implicitly attempt to account for the effects of chain stiffness and cohesive forces. One such correlation is the familiar relationship of van Krevelen (31) based on group contributions. Many other empirical correlations, which also usually express T_g as a function of quantities calculated via group contributions, have been used with limited success. A review article (32) provides detailed quantitative critical assessments, and extensive lists of the original references, for some of the best-known empirical correlations for T_g. Some of the many other interesting attempts to estimate T_g, which were not reviewed (32), include the method of Askadskii and Slonimskii (33,34), an alternative version of this method developed by Wiff and co-workers (35), and the combination of molecular modeling and group contributions in the method of Hopfinger and co-workers (36).

More recently, new quantitative structure–property relationships for T_g have been developed (1); they are based on the statistical analysis of experimental data for 320 linear (uncross-linked) polymers collected from many different sources, containing a vast variety of compositions and structural features. The T_g of the atactic form was used, whenever available, for polymers manifesting different tacticities. The T_g values of a subset of the polymers listed in this extensive tabulation are reproduced (with some minor revisions) in Table 1. (It is important to caution the reader here that these data were assembled from a wide variety of sources. Many different experimental techniques were used in obtaining these data.) The resulting relationship for T_g has the form of a weighted sum of "structural terms" mainly taking the effects of chain stiffness into account plus a term proportional to the solubility parameter δ which takes the effects of cohesive interchain interactions in an explicit manner, as shown in equation (1):

$$T_g \approx a + b\cdot\Delta + (\text{weighted sum of 13 structural terms}) \qquad (1)$$

Literature data for the dependence of T_g on the number-average molecular weight (M_n) were also tabulated in Reference 1, and used to develop a quantitative structure–property relationship for the fitting parameter K_g in equation (2) (developed from considerations of free volume) where $T_{g\infty}$ is the limiting value of T_g for $M_n \rightarrow \infty$ (37). As shown for poly(ethylene terephthalate) in Figure 6 (38), T_g increases asymptotically toward $T_{g\infty}$ with increasing M_n. $T_{g\infty}$ is often larger than the commonly quoted T_g of a polymer, as measured at ordinary molecular weights. For example, $T_{g\infty} \approx 382$ K for polystyrene and $T_{g\infty} \approx 434$ K for bisphenol A polycarbonate, in comparison with the commonly quoted values of $T_g \approx 373$ K and $T_g \approx 423$ K, respectively. A subset of the data tabulated elsewhere (1) for the dependence of T_g on M_n, as fitted by using equation (2), is listed in Table 2. The final form of the resulting quantitative structure–property relationship is given by

Table 1. Glass-Transition Temperatures (T_g) of Some Polymers[a]

Polymer	T_g, K	Polymer	T_g, K
Poly(dimethyl siloxane)	152	Poly(vinyl butyral)	324
Poly(1,4-butadiene)	171	Poly(ethylene isophthalate)	324
Polyoxytetramethylene	190	Poly(ethyl methacrylate)	324
Polyisobutylene	199	Poly(*sec*-butyl methacrylate)	330
Polyisoprene	203	Poly(hexamethylene adipamide)	330
Poly(tetramethylene adipate)	205	Poly(*p*-xylylene)	333
Polyoxyethylene	206	Poly(ε-caprolactam)	335
Poly(propylene oxide)	206	Poly(ethylene terephthalate)	345
Poly(ε-caprolactone)	213	Poly(vinyl chloride)	348
Poly(decamethylene adipate)	217	Poly(vinyl alcohol)	358
Polyoxymethylene	218	Poly[oxy(*p*-phenylene)]	358
Poly(dodecyl methacrylate)	218	Poly(2-hydroxyethyl methacrylate)	359
Poly(*n*-butyl acrylate)	219	Polystyrene	373
Poly(vinyl *n*-butyl ether)	221	Phenoxy resin	373
Poly(1-hexene)	223	Poly(cyclohexyl methacrylate)	377
Polychloroprene	225	Poly(methyl methacrylate)	378
Poly(1-butene)	228	Polyacrylonitrile	378
Poly(ethylene adipate)	233	Poly(acrylic acid)	379
Poly(isobutyl acrylate)	249	Polymethacrylonitrile	393
Poly(ethyl acrylate)	251	Poly(ethylene-2,6-naphthalenedicarboxylate)	397
Poly(*n*-octyl methacrylate)	253	Poly(*p*-*t*-butyl styrene)	402
Poly(vinylidene chloride)	256	Poly(hexamethylene isophthalamide)	403
Polypropylene	266	Poly(*o*-methyl styrene)	409
Poly(*n*-hexyl methacrylate)	268	Poly(α-methyl styrene)	409
Poly(1,2-butadiene)	269	Poly(*m*-phenylene isophthalate)	411
Poly(*p*-*n*-butyl styrene)	279	Poly(*p*-vinylpyridine)	415
Poly(methyl acrylate)	281	Poly(*N*-vinylpyrrolidinone)	418
Poly(*n*-butyl methacrylate)	293	Poly(*p*-hydroxybenzoate)	420
Poly(vinyl acetate)	301	Bisphenol A polycarbonate	423
Poly(4-methyl-1-pentene)	302	Poly(*N*-vinyl carbazole)	423
Poly(12-aminododecanoic acid)	310	Poly(α-vinyl naphthalene)	432
Poly(hexamethylene sebacamide)	313	Poly(bisphenol A terephthalate)	478
Poly(10-aminodecanoic acid)	316	Poly[oxy(2,6-dimethyl-1,4-phenylene)]	482
Poly[oxy(*m*-phenylene)]	318	Poly[4,4′-diphenoxy di(4-phenylene)sulfone]	493
Poly(isobutyl methacrylate)	321	Poly(*m*-phenylene isophthalamide)	545
Poly(8-aminocaprylic acid)	324	Poly(*p*-phenylene terephthalamide)	600

[a]Data presented here are a part of literature data summarized in Ref. 1.

equation (3), which is illustrated in Figure 7. Other (more complex) relationships for the M_n dependence of T_g, which work better than equation (3) for polymers with a vinyl-type chain backbone, are also available and have been reviewed elsewhere (1).

$$T_g \approx T_{g\infty} - \frac{K_g}{M_n} \tag{2}$$

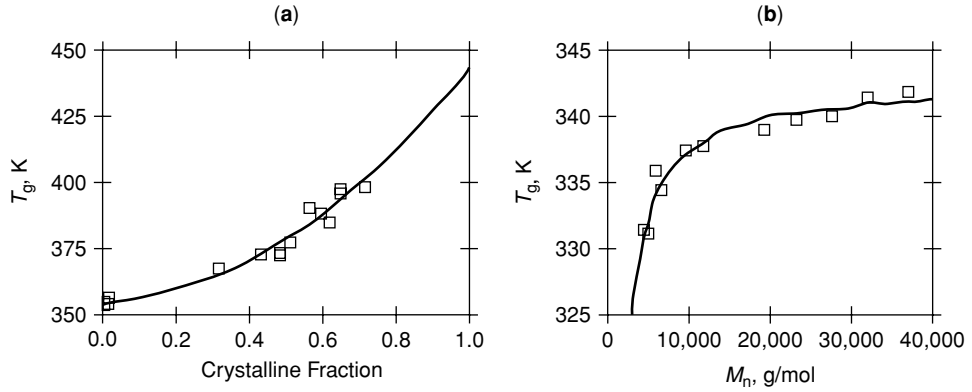

Fig. 6. Experimental data collected from the literature and empirical fits to these data, for the T_g of poly(ethylene terephthalate) (38), as a function of (a) crystalline fraction, and (b) M_n.

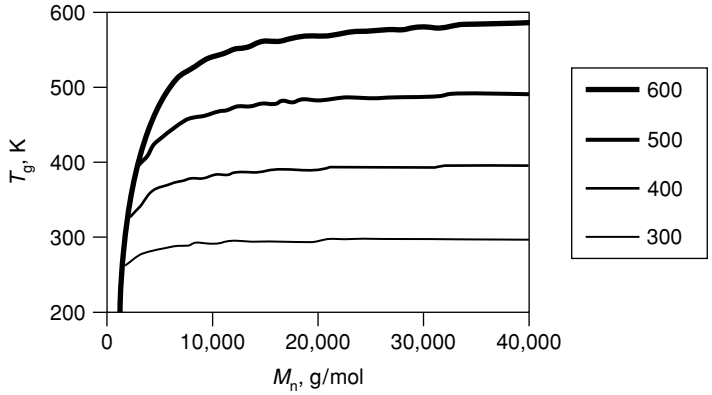

Fig. 7. Illustration of simple quantitative structure–property relationship given by equation (3) for the M_n dependence of T_g. Each curve is labeled by the value of $T_{g\infty}$, which is the limiting value of T_g for $M_n \to \infty$. More accurate relationships are also available for vinylic polymers.

$$T_g \approx T_{g\infty} - 0.002715\frac{T_{g\infty}^3}{M_n} \tag{3}$$

Many commercial polymers are cross-linked, ranging from lightly cross-linked elastomers to very densely cross-linked thermosets. The effects of crosslinking on the properties of polymers can be roughly classified as follows (40,41): (*1*) *Topological effect* caused by topological constraints introduced by cross-links on the properties. This effect is referred to simply as the *cross-linking effect* by many authors. (*2*) *Copolymerization effect* (also referred to as the *copolymer effect*) related to the change of the fractions of two or more types of repeat units with increasing cross-linking. Depending on the types of monomers involved, this effect may either strengthen or weaken the trends expected on the basis of the topological

Table 2. Dependence of T_g on M_n as fitted by the Parameter K_g of Equation (2)[a]

Polymer	K_g, 10^4 k·g/mol	$T_{g\infty}$, K
Poly(dimethyl siloxane)	0.6	150
n-Alkanes	1.2	176
Polyisoprene	1.2	207
Polybutadiene	1.2	174
Poly(ethylene adipate)	1.3	228
Poly(propylene oxide)	2.5	198
Polypropylene	3.9	266
Poly(tetramethylene terephthalate)	4.6	295
Poly(ethylene terephthalate)	5.1	342
Polyisobutylene	6.4	243
Poly(vinyl acetate)	8.9	305
Isotactic poly(methyl methacrylate)	11.0	318
Poly(glycidyl methacrylate)	11.3	350
Poly(vinyl chloride)	12.3	351
Polyacrylonitrile	14.0	371
Bisphenol A polycarbonate	18.7	434
Polystyrene	20.0	382
Atactic poly(methyl methacrylate)	21.0	388
Poly(*N*-vinyl carbazole)	22.8	500
Syndiotactic poly(methyl methacrylate)	25.6	405
Poly(*p*-methylstyrene)	26.5	384
Syndiotactic poly(α-methylstyrene)	31.0	453
Atactic poly(α-methylstyrene)	36.0	446
Poly(*p*-tert-butylstyrene)	38.5	430

[a]Data presented here are a part of literature data summarized in Ref. 1 (see Ref. 39 for a more extensive discussion) to develop a relationship for the parameter K_g in equation (2).

effect, and may even reverse them in some cases. The analysis of a large amount of experimental data collected from the literature [(1); for a more detailed discussion see (39)] led to the simple quantitative structure–property relationship given by equation (4) (illustrated in Fig. 8), where n (defined by eq. (5)) is the average number of "repeat units" between cross-links. M_c is the average molecular weight between cross-links. M is the molecular weight per repeat unit. $T_g(\infty)$ is T_g at the uncross-linked limit ($n\rightarrow\infty$). N_{rot} is a "number of rotational degrees of freedom per repeat unit" parameter.

$$T_g(n) \approx T_g(\infty)\left[1+\frac{5}{n\times N_{rot}}\right] \tag{4}$$

$$n=\frac{M_c}{M} \tag{5}$$

In many phase-separating block copolymers (especially segmented multiblock copolymers such as polyurethanes where the blocks are usually short), lowering the soft block M_n *increases* the soft phase T_g because of "cross-link-like" topological constraints imposed by hard phase domains.

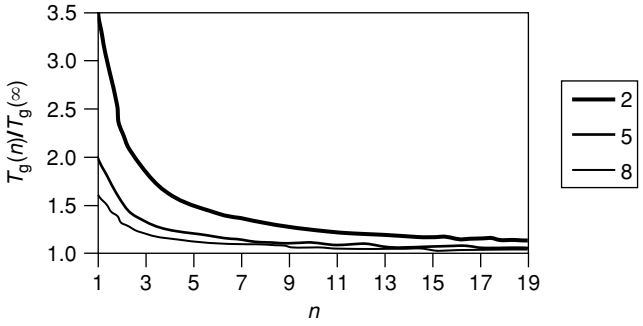

Fig. 8. Illustration of simple quantitative structure–property relationship given by equation (4) for the dependence of T_g on cross-linking. $T_g(\infty)$ is the T_g of the uncross-linked limit ($n \to \infty$, where n is the number of repeat units between cross-links). N_{rot} is a "number of rotational degrees of freedom per repeat unit" parameter. Each curve is labeled by the value of N_{rot}.

Other recently published correlative methods for predicting T_g include the "group interaction modeling" (GIM) approach of Porter (42), neural networks (43–45), genetic function algorithms (46), the CODESSA (acronym for "Comprehensive Descriptors for Structural and Statistical Analysis") method (47), the "energy, volume, mass" (EVM) approach (48,49), correlation to the results of semiempirical quantum mechanical calculations of the electronic structure of the monomer (50), and a method that combines a thermodynamic equation-of-state based on lattice fluid theory with group contributions (51).

Most theories and quantitative structure–property relationships for T_g only consider the case of a random distribution of repeat units along the polymer chains in treating copolymers. They give equations which predict a monotonic change of T_g between the T_g values of the homopolymers of the constituent repeat units, as a function of composition. However, the distribution of repeat units in a copolymer is often nonrandom. It may, for example, manifest various levels of "blockiness." Sometimes, T_g shows a nonmonotonic dependence on the composition variables, usually as a result of deviations of the repeat unit sequence from complete randomness. Some developed useful relationships correlating the T_g of a copolymer to the sequence of its repeat units have been developed (52). See also a review by Schneider (53), dealing with the deviations of T_g from simple additive relationships for copolymers and miscible polymer blends, and a review by Cowie and Arrighi (54), discussing the glass transition and sub-T_g relaxations in blends in greater depth. It should also be noted that sometimes nonmonotonic dependence of T_g on copolymer composition may arise as a result of preferential ("specific") types of nonbonded interactions (such as polar interactions and hydrogen bonding) between certain types of repeat units causing nonmonotonic composition dependence for the cohesive energy density. It has been shown that the differences between the solubility parameters (square root of the cohesive energy density) of the components of a random copolymer or a miscible blend can be correlated with the magnitude of such effects (53). In the context of experimental data for copolymers of vinylidene chloride, it has been shown how "the T_g-composition relationship is affected by four distinct structural features: the size, shape, and polarity of the comonomer unit, and the sequence distribution" (55).

It is important to note that quantitative structure–property relationships for T_g (as well as for other polymer properties) can be combined with nonlinear optimization techniques to perform "reverse engineering." These approaches involve working backwards, from a desired set of properties toward the repeat unit structures of the polymers that may give those targeted properties. See References 56–58 for some examples.

Detailed Simulations

In recent years, the rapidly increasing power of computational hardware and software has encouraged attempts to study the glass transition by fully atomistic or coarse-grained numerical simulations. Such simulations can be used to probe details of the physical processes taking place in a system at length scales, which cannot be probed by thermodynamic and kinetic theories which are based on a more "global" description of the system at larger length scales. Some of the details that can be probed by such simulations are also not accessible by any of the existing experimental techniques. Simulations have already begun producing valuable physical insights.

An objective of such work is to predict T_g by identifying the temperature at which discontinuities occur in the properties obtained directly from the results of the simulations. The results obtained thus far are insufficient to demonstrate conclusively the ability to accomplish this task routinely and reliably within computer time requirements that would be acceptable for the practical use of detailed simulations to predict T_g. The main challenge, at a fundamental level, is that the time scales involved in the glass transition are very long compared to what can currently be explored routinely in simulations on model systems large enough to represent a bulk polymer sample adequately and sufficiently fine-grained to account adequately for the effects of differences in chemical structure. Another significant challenge, at the implementation level, is the difficulty of developing potential functions (often referred to as "force fields") of sufficient quality to provide faithful representations of the properties and dynamics of the materials of interest. Significant progress is expected in coming years with further improvements in computer hardware and simulation software. It may, ultimately, become possible to use detailed simulations to predict reliably the effects of subtle variations in polymeric structure and conformation, which are very difficult to capture either with theoretical equations based on "global" thermodynamic and kinetic considerations or with empirically based relationships.

For further information, see the following four especially interesting articles:

(1) A review article (59) on the prediction of T_g by extending volume–temperature curves generated by molecular dynamics simulations to low temperatures.

(2) A study of the question of whether computer simulation can solve the challenge of understanding the glass transition and the amorphous state of matter (60).

(3) Molecular dynamics simulations of the thermal properties of ultrafine polyethylene powders (61). This study shows that, for particle diameters below 10 nm, both T_g and T_m are expected to decrease rapidly with decreasing particle diameter.

(4) Isobaric (constant pressure) and isochoric (constant volume) glass transitions in polymers were first observed for bisphenol A polycarbonate (62). A molecular dynamics study of such transitions in a model amorphous polymer has also been reported (63). This study shows that the glass transition is primarily associated with the freezing of the torsional degrees of freedom of polymer chains (related to chain stiffness), which are strongly coupled to the degree of freedom associated with the nonbonded Lennard–Jones potential (related to interchain cohesive forces).

Comprehensive List of Factors Determining T_g

Several of the most important factors determining the value of T_g have been discussed earlier:

(1) *Rate of measurement*
(2) *Structural and compositional factors*—the most fundamental of which are *chain stiffness* and interchain *cohesive forces*
(3) *Number-average molecular weight*
(4) *Cross-linking*

The following are the additional factors which affect the value of T_g:

(1) Morphological effects, and especially *crystallinity*.
   a. The presence of the rigid crystallites, and of the interphase regions ("tie molecules") between amorphous and crystalline regions, often increases T_g (1,38,64), as shown for poly(ethylene terephthalate) in Figure 6 (38). In addition, the decrease of the amorphous fraction of the polymer naturally leads to a decrease in the strength (intensity) of its amorphous relaxations, with the decrease in the strength of the glass transition at a given percent crystallinity normally being larger than the decrease in the strength of the secondary (sub-T_g) relaxations (65). The increase in T_g due to crystallinity bears some resemblance to the increase in T_g due to cross-linking, so that it can be viewed somewhat superficially to arise from the topological constraints introduced by the crystallites. This simple physical picture, however, is not entirely correct. Unlike a crosslink in an amorphous polymer, which can be viewed as a "point-like" network junction, a crystalline domain in a semicrystalline polymer can be very large, such domains can occupy a very large fraction of the total volume of the specimen, and they often transition into the amorphous phase gradually via "interphase" regions of significant thickness. It has, therefore, not yet proved to be possible to develop any simple and statistically significant general quantitative structure–property relationship for the

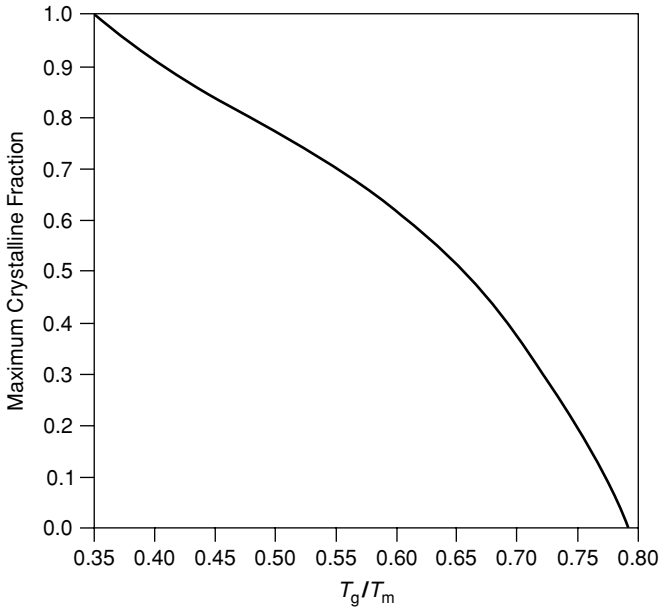

Fig. 9. Empirical relationship for maximum crystalline fraction under isothermal quiescent crystallization as a function of the ratio T_g/T_m, where the temperatures are in Kelvin.

effects of crystallinity on T_g, unlike equation (4) which works quite well in describing the effects of cross-linking.

b. While crystallinity influences T_g, T_g in turn influences the crystallization of a polymer when it is cooled down from the melt (38). The temperature at which the isothermal quiescent crystallization rate is at its maximum is roughly halfway between T_g and T_m. The maximum crystalline fraction increases with increasing T_m/T_g (with temperatures expressed in Kelvin) which can be viewed as an index for the driving force for crystallization, and thus decreases with increasing T_g/T_m as shown in Figure 9. A very important physical difference between T_g and T_m is worth noting in this context. They both depend strongly on chain stiffness and on cohesive energy density, *but* only T_m depends on how easily polymer chains can be packed into a periodic lattice. Otherwise, the T_m/T_g ratio and crystallizability would have been very similar for all polymers, instead of depending strongly on the smoothness and regularity of polymer chains.

(2) The effects of *orientation* via mechanical deformation on T_g have been reviewed (64). T_g increases in those amorphous regions of a semicrystalline polymer that are either attached to crystallites or so close to them that their chain segment mobilities are hindered because of the interference of the crystallites. On the other hand, orientation has little effect on T_g in amorphous regions far away from crystallites as well as in completely amorphous polymers.

Table 3. Glass-Transition Temperatures of Syndiotactic, Isotactic, and Atactic Polymers[a]

Polymer	T_g (syndiotactic), K	T_g (isotactic), K	T_g (atactic), K
Poly(methyl methacrylate)	433	316	378
Poly(ethyl methacrylate)	393	281	324
Poly(isopropyl methacrylate)	412	300	327
Poly(*n*-butyl methacrylate)	361	249	293
Poly(isobutyl methacrylate)	393	281	321
Poly(cyclohexyl methacrylate)	436	324	377
Poly(2-hydroxyethyl methacrylate)	377	308	359
Poly(methyl acrylate)	–	283	281
Poly(ethyl acrylate)	–	248	249
Poly(isopropyl acrylate)	270	262	267
Poly(*sec*-butyl acrylate)	–	250	251
Poly(cyclohexyl acrylate)	–	285	292
Poly(methyl α-chloroacrylate)	450	358	416
Poly(ethyl α-chloroacrylate)	393	310	366
Poly(isopropyl α-chloroacrylate)	409	341	363
Polystyrene	378	360	373
Poly(α-methyl styrene)	453	–	446
Polypropylene	269	255	267
Poly(*N*-vinyl carbazole)	549	399	423
Poly(vinyl chloride)	T_g increased with syndiotactic triad content (28–43%), and decreased with isotactic triad content (13–21%) showing lowest and highest values of 352 and 370 K, respectively, for a set of samples.		

[a]Data presented here are a part of literature data summarized in Ref. 1.

(3) *Conformational factors*. The most important conformational factor is the *tacticity* of vinyl-type polymers. A polymer such as poly(methyl methacrylate) can have quite different values of T_g, depending on whether it is isotactic, syndiotactic, or atactic. See Table 3 for a collection of literature data (1) on the effects of tacticity on T_g. A theoretical analysis of the effects of tacticity variations on T_g has been provided (52).

(4) The presence of *additives, fillers, unreacted residual monomers, and/or impurities*, whether deliberately included in the formulation of a resin, or left over as undesirable by-products of synthesis. For example, plasticizers of low molecular weight generally decrease T_g (1,19,31,66,67), as illustrated in Figure 10. On the other hand, under some conditions, T_g may increase when rigid nanoscale additives are incorporated into a polymer (64).

(5) *Thermal history*. The annealing (or "physical aging") of amorphous polymers at elevated temperatures below T_g usually increases T_g. This increase is larger for higher annealing temperatures, provided that the annealing temperature remains below T_g. It approaches an asymptotic limit as a function of time. For example, see Reference 68 for bisphenol A polycarbonate and Reference 64 for amorphous rigid poly(vinyl chloride).

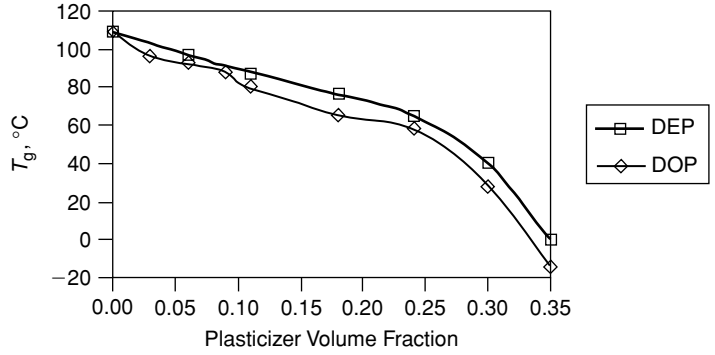

Fig. 10. Data illustrating typical effects of plasticization on T_g (67) for poly(methyl methacrylate) (obtained by polymerization of purified methyl methacrylate monomer), plasticized with diethyl phthalate (DEP) or dioctyl phthalate (DOP).

(6) *Thermal, thermooxidative, and/or photochemical degradation*. The onset of rapid degradation sometimes occurs in the temperature range of the glass transition, obscuring the distinction between the glass transition and degradation. For example, T_g values of 700 K or above, reported in the literature for some polymers with very stiff chains, are often not true T_g values, since degradation and softening take place simultaneously and inextricably.

(7) *Pressure* (P). T_g is usually measured under normal atmospheric pressure. The effect of P on T_g is rarely considered, although it may become important in processing polymers under high hydrostatic pressure. Increasing P increases T_g (19,63,64,69,70). The observed rate of change of T_g with increasing P (the derivative dT_g/dP) seems to be of the same order of magnitude for many polymers. The following examples from a tabulation of literature data (64) illustrate the typical magnitude of this effect: T_g went from (a) 100°C at atmospheric pressure (P_{atm}) to 182°C for polystyrene at P=200 MPa, (b) 103°C at P_{atm} to 121°C at P=100 MPa for poly(methyl methacrylate), (c) 75°C for poly(vinyl chloride) at P_{atm} to 89°C at P=100 MPa, and (d) 31.5°C at P_{atm} to 48.5°C at P=80 MPa for poly(vinyl acetate).

(8) *Specimen size effects*.

a. Sometimes, as in many electronics and lubrication applications, very thin polymeric films are used. The T_g values of such films can differ significantly from the bulk values for the same polymers (71–76). It was shown that T_g decreases with decreasing thickness for thin free-standing polystyrene films (71). T_g also decreases with decreasing thickness for polymers that have no specific interactions with the substrate on which they have been placed (72), as shown in Figure 11. By contrast, if strong attractive specific interactions between the polymer and the substrate restrict the mobility in the interfacial region, the behavior becomes very different and T_g may increase with decreasing thickness (73,74).

b. The surface of a polymeric specimen may behave differently from the bulk in its glass-transition behavior. For example (75), the surface T_g of a monodisperse polystyrene film was observed to be lower than the

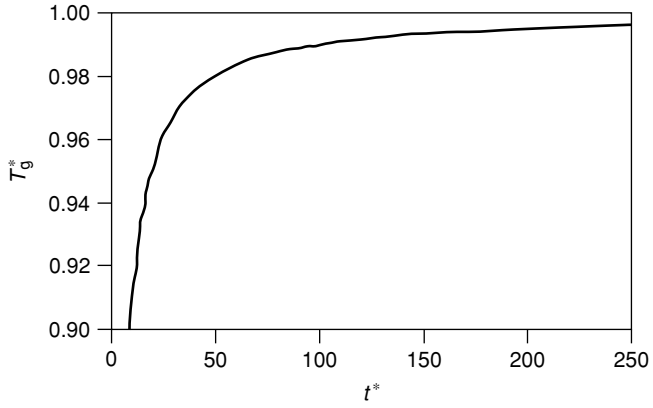

Fig. 11. "Master curve" for thickness (t) dependence of T_g of thin films of polymers that have no specific interactions with the substrate (72). The equation for the curve is $T_g* = t*/(1+t*)$; where $T_g* = T_g(t)/T_g(\text{bulk})$, T_g is in Kelvin, $t* = t/L$, and L is the statistical chain (Kuhn) segment length. By contrast, if strong specific interactions between the polymer and the substrate result in restricted interfacial region mobility, the behavior becomes very different from what is shown below and T_g may instead increase with decreasing thickness.

bulk T_g. This result was interpreted in terms of an increase in the free volume near the surface region, being induced by the preferential surface localization of chain end groups.

c. Finite specimen size, resulting from confinement within small spaces, can also affect T_g significantly. For example, it has been observed that the T_g of two glass-forming organic liquids decreased (but not as much as the decrease of T_m) when the confining controlled pore glass diameter decreased over the range of 73–4 nm (77,78).

(9) *Incorporation of ionic charges*. An ionic polymer (sometimes referred to as an "ionomer") contains both covalent and ionic bonds in its chain or network structure (79,80). Examples include metal salts of poly(acrylic acid), poly(styrene-*co*-methacrylic acid), and sulfonated polystyrene. The effect of ionic bonds on T_g somewhat resembles the effect of covalent cross-links for organic polymers, as T_g generally increases with ion concentration. However, ionic bonding is more complex than covalent cross-linking, because of the possible effects of (*1*) ionic valency, (*2*) chain stiffening induced by incorporating ionic charges along the chain backbone, (*3*) ionic aggregation, and (*4*) thermal lability of "ionic cross-links."

This long list of factors affecting T_g demonstrates that many factors not related either to the composition or to the structure of a polymer can significantly affect T_g. Some internal inconsistency, and the need to exercise judgment and to make choices, is therefore inherent in preparing any data set collected from different sources for use in developing or validating any correlative or predictive scheme for T_g. In the best of all possible worlds, one would synthesize all of the polymers which will be used in the dataset, characterize them very carefully, and

then measure their T_g's under identical test conditions. For practical reasons, however, the use of data from many different sources in examining the trends in T_g is often unavoidable.

A review article (81) provides further insights into the many factors determining T_g.

BIBLIOGRAPHY

"Glass Transition" in *EPST* 1st ed., Vol. 7 p. 461; "Glass Transition" in *EPSE* 2nd ed., Vol. 7, pp. 531–544, by R. J. Roe, University of Cincinnati.

1. J. Bicerano, *Prediction of Polymer Properties*, 2nd ed., Marcel Dekker, Inc., New York, 1996.
2. D. J. Meier, ed., *Molecular Basis of Transitions and Relaxations*, Gordon and Breach Science Publishers, London, 1978.
3. M. T. Takemori, *Polym. Eng. Sci.* **19**, 1104–1109 (1979).
4. S. Krause, in D. R. Paul and S. Newman, eds., *Polymer Blends*, Vol. **1**, Academic Press, New York, 1978, pp. 15–112.
5. G. Holden, N. R. Legge, R. P. Quirk, and H. E. Schroeder, eds., *Thermoplastic Elastomers*, 2nd ed., Hanser Publishers, Munich, 1996.
6. B. K. Kim, S. Y. Lee, and M. Xu, *Polymer* **37**, 5781–5793 (1996).
7. S. Hayashi, in K. Inoue, S. I. Y. Shen, and M. Taya, eds. *US–Japan Workshop on Smart Materials and Structures*, The Minerals, Metals and Materials Society, Warrendale, Pa., 1997, pp. 29–38.
8. V. A. Bershtein and V. M. Yegorov, *Polym. Sci. USSR* **27**, 2743–2757 (1985).
9. V. A. Bershtein, V. M. Yegorov, and Yu. A. Yemel'yanov, *Polym. Sci. USSR* **27**, 2757–2764 (1985).
10. P. J. Flory, *The Principles of Polymer Chemistry*, Cornell University Press, Ithaca, N.Y., 1953.
11. P. J. Flory, *Statistical Mechanics of Chain Molecules*, Wiley-Interscience, New York, 1969.
12. R. Zallen, *The Physics of Amorphous Solids*, John Wiley & Sons, Inc., New York, 1983.
13. J. Bicerano and D. Adler, *Pure Appl. Chem.* **59**, 101–144 (1987).
14. J. H. Gibbs and E. A. DiMarzio, *J. Chem. Phys.* **28**, 373–383 (1958).
15. E. A. DiMarzio and J. H. Gibbs, *J. Chem. Phys.* **28**, 807–813 (1958).
16. G. Adam and J. H. Gibbs, *J. Chem. Phys.* **43**, 139–146 (1965).
17. R. P. Kusy and A. R. Greenberg, *Polymer* **23**, 36–38 (1982).
18. A. R. Greenberg and R. P. Kusy, *Polymer* **24**, 513–518 (1983).
19. P. R. Couchman, *Polym. Eng. Sci.* **24**, 135–143 (1984).
20. M. Goldstein, *Ann. N.Y. Acad. Sci.* **279**, 68–77 (1976).
21. M. Goldstein, *J. Chem. Phys.* **64**, 4767–4774 (1976).
22. G. P. Johari, in B. Escaig and C. G. Sell, eds., *Plastic Deformation of Amorphous and Semicrystalline Materials*, "Les Houches Lectures, Les Editions de Physique", 1982, pp. 109–141.
23. M. H. Cohen and G. S. Grest, *Phys. Rev. B* **20**, 1077–1098 (1979).
24. G. S. Grest and M. H. Cohen, *Adv. Chem. Phys.* **48**, 455–525 (1981).
25. H. Stutz, K.-H. Illers, and J. Mertes, *J. Polym. Sci., Polym. Phys. Ed.* **28**, 1483–1498 (1990).
26. C. A. Angell, *J. Non-Cryst. Solids* **131–133**, 13–31 (1991).
27. C. A. Angell, *Science* **267**, 1924–1935 (1995).
28. C. A. Angell, *ACS Symp. Ser.* **710**, 37–52 (1998).

29. H. Sillescu, *J. Non-Cryst. Solids* **243**, 81–108 (1999).
30. G. B. McKenna and S. C. Glotzer, eds., *J. Research National Institute of Standards and Technology* **102**(2 Special Issue: 40 Years of Entropy and the Glass Transition) (Mar.–Apr. 1997).
31. D. W. van Krevelen, *Properties of Polymers*, 3rd ed., Elsevier, Amsterdam, 1990.
32. C. J. Lee, *J. Macromol. Sci., C: Rev. Macromol. Chem. Phys.* **29**, 431–560 (1989).
33. A. A. Askadskii and G. L. Slonimskii, *Polym. Sci. USSR* **13**, 2158–2160 (1971).
34. A. A. Askadskii, *Physical Properties of Polymers: Prediction and Control*, Gordon and Breach, New York, 1996.
35. D. R. Wiff, M. S. Altieri, and I. J. Goldfarb, *J. Polym. Sci., Polym. Phys. Ed.* **23**, 1165–1176 (1985).
36. A. J. Hopfinger and co-workers, *J. Polym. Sci. Polym. Phys. Ed.* **26**, 2007–2028 (1988).
37. T. G. Fox and P. J. Flory, *J. Appl. Phys.* **21**, 581–591 (1950).
38. J. Bicerano, *J. Macromol. Sci., C: Rev. Macromol. Chem. Phys.* **38**, 391–479 (1998).
39. J. Bicerano and co-workers, *J. Polym. Sci., Polym. Phys. Ed.* **34**, 2247–2259 (1996).
40. T. G. Fox and S. Loshaek, *J. Polym. Sci.* **15**, 371–390 (1955).
41. S. Loshaek, *J. Polym. Sci.* **15**, 391–404 (1955).
42. D. Porter, *Group Interaction Modelling of Polymer Properties*, Marcel Dekker, Inc., New York, 1995.
43. B. G. Sumpter and D. W. Noid, *Macromol. Theory Simul.* **3**, 363–378 (1994).
44. C. W. Ulmer II and co-workers, *Comput. Theor. Polym. Sci.* **8**, 311–321 (1998).
45. E. R. Collantes and co-workers, *Antec '97 Preprints* 2245–2248 (1997).
46. D. Rogers and A. J. Hopfinger, *J. Chem. Inf. Comput. Sci.* **34**, 854–866 (1994).
47. A. R. Katritzky and co-workers, *J. Chem. Inf. Comput. Sci.* **38**, 300–304 (1998).
48. P. Camelio and co-workers, *J. Polym. Sci., Polym. Chem. Ed.* **35**, 2579–2590 (1997).
49. P. Camelio and co-workers, *Macromolecules* **31**, 2305–2311 (1998).
50. T. T. M. Tan and B. M. Rode, *Macromol. Theory Simul.* **5**, 467–475 (1996).
51. D. Boudouris, L. Constantinou, and C. Panayiotou, *Fluid Phase Equilib.* **167**, 1–19 (2000).
52. H. Suzuki, N. Kimura, and Y. Nishio, *J. Therm. Anal.* **46**, 1011–1020 (1996).
53. H. A. Schneider, *J. Therm. Anal. Calorim.* **56**, 983–989 (1999).
54. J. M. G. Cowie and V. Arrighi, *Plast. Eng. (N.Y.)* **52** (Polymer Blends and Alloys) 81–124 (1999).
55. R. A. Wessling and co-workers, *Appl. Polym. Symp.* **24**, 83–105 (1974).
56. R. Vaidyanathan and M. El-Halwagi, *Ind. Eng. Chem. Res.* **35**, 627–634 (1996).
57. C. D. Maranas, *Ind. Eng. Chem. Res.* **35**, 3403–3414 (1996).
58. C. D. Maranas, *AIChE J.* **43**, 1250–1264 (1997).
59. R. H. Boyd, *Trends Polym. Sci.* **4**, 12–17 (1996).
60. K. Binder, *Comput. Phys. Commun.* **121/122**, 168–175 (1999).
61. K. Fukui and co-workers, *Macromol. Theory Simul.* **8**, 38–45 (1999).
62. D. M. Colucci and co-workers, *J. Polym. Sci, Polym. Phys. Ed.* **35**, 1561–1573 (1997).
63. L. Yang, D. J. Srolovitz and A. F. Yee, *J. Chem. Phys.* **110**, 7058–7069 (1999).
64. S. M. Aharoni, *Polymers for Advanced Technologies* **9**, 169–201 (1998).
65. T. Alfrey Jr. and R. F. Boyer, in Ref. 2, pp. 193–202.
66. J. K. Sears and J. R. Darby, *The Technology of Plasticizers*, John Wiley & Sons, Inc., New York, 1982.
67. S. Kalachandra and D. T. Turner, *J. Polym. Sci., Polym. Phys. Ed.* **25**, 1971–1979 (1987).
68. K. Neki and P. H. Geil, *J. Macromol. Sci., B: Phys.* **8**, 295–341 (1973).
69. R. W. Warfield and B. Hartmann, *Polymer* **23**, 1835–1837 (1982).
70. S. Saeki and co-workers, *Polymer* **33**, 577–584 (1992).
71. J. R. Dutcher, K. Dalnoki-Veress, and J. A. Forrest, *ACS Symp. Ser.* **736**, 127–139 (1999).

72. J. H. Kim, J. Jang, and W.-C. Zin, *Langmuir* **16**, 4064–4067 (2000).
73. J. L. Keddie, R. A. L. Jones, and R. A. Cory, *Faraday Discuss.* **98**, 219–230 (1994).
74. W. E. Wallace, J. H. van Zanten, and W. L. Wu, *Phys. Rev. E* **52**, R3329–R3332 (1995).
75. T. Kajiyama and co-workers, *Macromol. Symp.* **143**, 171–183 (1999).
76. J. Ral, *Curr. Opin. Colloid Interface Sci.* **4**, 153–158 (1999).
77. C. L. Jackson and G. B. McKenna, *J. Non-Cryst. Solids* **131–133**, 221–224 (1991).
78. C. L. Jackson and G. B. McKenna, *Chem. Mater.* **8**, 2128–2137 (1996).
79. L. Holliday, in L. Holliday, ed., *Ionic Polymers*, John Wiley & Sons, Inc., New York, 1975, pp. 1–68. The glass transition in ionic polymers is discussed on pages 35–46.
80. C. W. Lantman, W. J. MacKnight, and R. D. Lundberg, *Annu. Rev. Mater. Sci.* **19**, 295–317 (1989).
81. D. J. Plazek and K. L. Ngai, in J. E. Mark, ed., *Physical Properties of Polymers Handbook*, American Institute of Physics, Woodbury, N.Y., 1996, pp. 139–159.

JOZEF BICERANO
The Dow Chemical Company